Colloids and Surfaces A: Physicochemical and Engineering Aspects 691 (2024) 133890

Contents lists available at ScienceDirect

Colloids and Surfaces A: Physicochemical and Engineering Aspects

journal homepage: www.elsevier.com/locate/colsurfa

Mechanical activation and silver supplementation as determinants of the antibacterial activity of titanium dioxide nanoparticles

Ljubica Andjelković [a], Marija Šuljagić [a], Vladimir Pavlović [b], Miljana Mirković [c], Boško Vrbica [d], Irena Novaković [a], Dalibor Stanković [d], Aleksandar Kremenović [e], Vuk Uskoković [f,g,*]

[a] University of Belgrade-Institute of Chemistry, Technology and Metallurgy, Department of Chemistry, Njegoševa 12, Belgrade, Serbia
[b] University of Belgrade, Faculty of Agriculture, Nemanjina 6, Belgrade, Serbia
[c] Department of Materials, "VINČA" Institute of Nuclear Sciences - National Institute of the Republic of Serbia, University of Belgrade, Belgrade, Serbia
[d] University of Belgrade, Faculty of Chemistry, Studentski Trg 12-16, Belgrade, Serbia
[e] Faculty of Mining and Geology, University of Belgrade, Djušina 7, Belgrade 11000, Serbia
[f] TardigradeNano LLC, Irvine, CA 92604, USA
[g] Department of Mechanical Engineering, San Diego State University, San Diego, CA 92182, USA

HIGHLIGHTS

- The mechanical activation of TiO_2 as an prerequisite for antibacterial activity
- Ag distribution over TiO_2 surface by ultrasonically-assisted chemical precipitation
- Homogeneous Ag deposition onto TiO_2 at a low net concentration
- The mechanical activation doubled the amount of Ag incorporable into TiO_2
- The mechanical activation and addition of Ag augmented TiO_2 antibacterial effect.

GRAPHICAL ABSTRACT

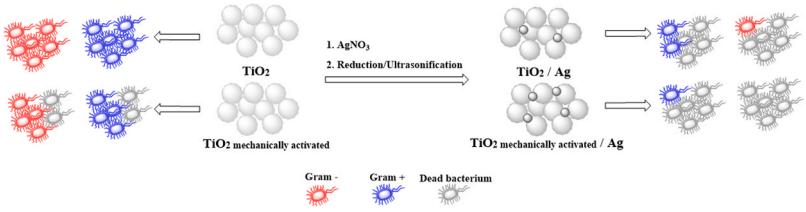

ARTICLE INFO

Keywords:
A. Composite materials
A. Inorganic materials
B. Precipitation
B. Mechanochemical processing
C. Microstructure

ABSTRACT

Metals and metal oxides have subpar antibacterial activities compared to those of small-molecule antibiotics, yet there are hopes that with proper compositional and structural adjustments this gap might be bridged. In this study, titanium dioxide (TiO_2) nanoparticles were mechanically activated and combined with particulate silver through simple reduction process elicited by UV irradiation and assisted with the ultrasound. The resulting powders in various combinations (Ag *vs.* no Ag, activated *vs.* non-activated) were characterized using a range of experimental techniques and assessed for their antibacterial activities. The preparation procedure presented in this work prevails over the disadvantages of many chemical routes, most critically by avoiding the use of toxic substances. The mechanical activation did not reduce the particle size or crystallinity of TiO_2 nor did it consistently alter the bandgap, yet it enabled the doubling of the amount of silver incorporable into the material. Further, while both mechanical activation and the addition of silver in the amount not exceeding 0.5 wt% produced barely detectable structural changes in the material, they both augmented its antibacterial activity. The precursor TiO_2 powder produced no inhibition zone against any of the four bacterial species tested, while the mechanical activation of TiO_2 led to the formation of distinct inhibition zones against each of the four bacterial species tested. The addition of silver to activated TiO_2 further widened the inhibition zones and it also imparted the antibacterial activity to non-activated TiO_2. The boost in the antibacterial activity achieved by the short

* Correspondence to: TardigradeNano LLC, Irvine, CA 92604, USA.
E-mail address: vuskokovic@sdsu.edu (V. Uskoković).

https://doi.org/10.1016/j.colsurfa.2024.133890
Received 22 November 2023; Received in revised form 30 March 2024; Accepted 1 April 2024
Available online 2 April 2024

mechanical activation was of a similar magnitude as the boost obtained after the addition of silver. The antibacterial activity was not different for different species when no silver was added to the system. However, with the addition of silver, species selectivity was obtained, as the composites were more effective against the two Gram-negative species (*Escherichia coli* and *Klebsiella pneumoniae*) than against the two Gram-positive ones (*Staphylococcus aureus* and *Bacillus subtilis*). The antibacterial activity increased with the addition of silver in the broth assay, but it was mediocre compared to that detected in the agar assay, attesting to the poor dispersability of the powders and their best performance when the bacterial cells migrate to the composite surface than *vice versa*. The findings of this study give hope that with appropriate microstructural or compositional alterations, the antibacterial activity of metal oxide powders and inorganic materials in general can be made comparable to that of small-molecule antibiotics.

1. Introduction

The astonishing ongoing progress in medicine allows for more effective treatments of most known diseases than it was possible only a few decades ago. On the other hand, the less developed regions are still dealing with high morbidities caused by bacterial and viral infections. Another serious threat to global public health that the modern society is facing comes in the form of the growing resistance of many pathogens to antibiotics [1–4]. According to the data acquired by the European Antimicrobial Resistance Surveillance Network (EARS-Net), the highest levels of resistance to antimicrobials were found in the countries of Southern and Eastern Europe [5]. To solve this problem, the World Health Organization (WHO) has been emphasizing the importance of finding suitable alternatives to traditional antibiotics for infection treatments [6].

Inorganic metal oxides have attracted a large scientific interest, not only as materials with a variety of applications in high technologies, but also as materials that could potentially address the health issues caused by the microbial resistance to antibiotics [7–10]. The antimicrobial performances of *3d* and alkaline earth metal oxides, such as ZnO [11–13], MgO [14–16], Fe_2O_3 [17–19], TiO_2 [20–23], and CuO [24–27], have been thoroughly studied in the past few years. Titanium dioxide (TiO_2) stands out among other metal oxides owing to its prominent catalytic activity, chemical stability, low cost, and mostly low to nil toxicity. Photocatalytic properties of TiO_2 are responsible for its antibacterial performance since the production of photoactivated reactive oxygen species (ROS) has been shown to cause the decomposition of the bacterial outer membranes, leading to phospholipid peroxidation and cell death [28]. Here, the main disadvantage of TiO_2 is a broad bandgap of approximately 3.2 eV, which limits its application to the UV region of the solar spectrum [29,30]. Since the UV region is a minor component of the solar spectrum, changing the band structure to increase the visible light sensitivity of TiO_2 is a strategy that could increase the antibacterial efficacy and enlarge the scope of application for TiO_2 as an antimicrobial. Recently, Pavlović et al. demonstrated that even short mechanical activation can exceptionally increase the visible light sensitivity of TiO_2 and enhance its antimicrobial activity [31]. Furthermore, mechanical activation, when sufficiently short, ensures that the formation of potentially adverse structural features, such as lattice defects, is avoided [32].

Doping is one of the most effective methods for solving the bandgap problem in metals [33–35]. Noble metals, especially silver, present a particularly favorable choice of dopants for this purpose [36–39]. It is well-known that silver, itself, shows pronounced antimicrobial properties [40–42]. The antibacterial activity of silver, moreover, is strongly affected by the particle size [43]. If the particles are smaller than 10 nm, silver ions are easily released, and are mainly responsible for the antimicrobial activity. In contrast, for larger silver particles (>20 nm), the antibacterial activity becomes increasingly dominated by the particle effects, considering that silver can bind to the bacterial cell membrane and damage it. Moreover, silver-thiol interactions in bacterial proteins cause the inactivation of respiratory enzymes. However, in spite of their prominent bactericidal activity, the application of bare Ag nanoparticles is questionable due to their toxicity to human cell lines [44–47], an effect that could be potentially mitigated through the formation of appropriate composites. Since Ag has a synergistic effect on TiO_2, many TiO_2/Ag composites were developed as advanced antimicrobial agents [29,30,48–52]. Among the many reported synthesis procedures [48,49,51,53], a simple physical reduction of silver cations over the TiO_2 surface stands out due to its simplicity and eco-friendly character. Simultaneously, the relatively mild conditions under which this chemical transformation is made to occur ensures that the desirable microstructural features of the material are preserved. The scientific community reports have drawn attention to such composites due to their significant antimicrobial activity and negligible toxicity to normal cells and tissues. Even when it is present at a very small concentration, silver reduces the TiO_2 bandgap, decreases the recombination of the charge carriers, and thus improves the sensitivity to visible light. Additionally, the antibacterial activity is also augmented by the capability of silver to destroy the bacterial cell wall.

The present study deals with the synthesis of an antimicrobial material based on nanocomposites containing anatase and silver nanoparticles. The anatase powder was mechanically treated using a short activation time in attempt to improve its antimicrobial activity. Further, the deposition of silver nanoparticles over the anatase surface, pristine and ball-milled, at a relatively low net concentration was conducted by employing a simple physical reduction of silver cations. Such a physical method enabled the optimization of the silver content, ensuring the avoidance of potential health hazards tied to the silver toxicity at higher concentrations. Moreover, and contrary to many chemical reduction methods, the photoreduction method applied was chosen to minimize the number of hazardous substances usually involved in such treatments. The synthesized materials were characterized with the use of X-ray powder diffraction (XRPD), the Fourier-transform infrared (FT-IR) spectroscopy, scanning electron microscopy (SEM) coupled with electron dispersive spectroscopy (EDS), and transmission electron microscopy (TEM). The silver content in the hetero-composites and the kinetics of its release were determined using inductively coupled plasma optical emission spectrometry (ICP-OES). The measurements of optical absorption properties were also performed. Anatase, the mechanically activated anatase, as well as hetero-nanocomposites containing these two forms of TiO_2 were investigated for their antibacterial activities against four distinct bacterial strains, two of which were Gram-positive and two of which were Gram-negative.

2. Material and methods

2.1. Material

All chemicals, including titanium dioxide (TiO_2 > 99.0% anatase) and silver nitrate ($AgNO_3$ > 99.0%),were obtained from Sigma-Aldrich (p.a. quality) and were used without additional purification. Deionized water was used in all experiments.

2.2. Synthesis

To enhance the antimicrobial activity, the commercially available (Sigma-Aldrich, 99.8%) TiO_2 powder (sample 1) was mechanically

activated in a planetary ball mill (Retsch $PM_{100}CM$) for 10 minutes, at 500 rpm, in a ZrO_2 jar with ZrO_2 balls that were 10 mm in diameter (the powder-to-ball ratio was 1:10), yielding sample 2. Mild milling conditions were chosen to prevent the negative effects related to prolonged activation times, such as lattice defects. For each sample, the deposition of silver was performed following the same procedure. TiO_2 in the amount of 1.5 g of was dispersed in 50 mL of a 1 wt.% $AgNO_3$ solution for 24 h. The obtained suspensions were ultrasonically treated for 8 h, while being exposed to UV radiation (Carl Roth GmbH, Karlsruge, Germany, $H_{469.1}$), using the Sankyo Denki (Tokyo, Japan) UV B lamp with the emission maximum of 312 nm and the flux of 7.7 J/m^2s. After the filtration, the precipitates were dried at ambient temperature and pulverized in the agate mortar, thus yielding samples 3 (TiO_2/Ag) and 4 (TiO_2 activated/Ag).

2.3. Characterization

An Ultima IV Rigaku diffractometer equipped with $CuK_{\alpha1,2}$ radiation was used for X-ray powder diffraction experiments. The generator voltage and the generator current used were 40 kV and 40 mA, respectively. The 2θ range between 10° and 120° was used in a continuous scan mode with a scanning step size of 0.02° and a scan rate of 5°/min, using D/TeX Ultra high - speed detector. The phase composition of the synthesized materials, the unit cell parameters and the size-strain values for anatase, as well as the phase abundances for anatase and rutile calculated by the relative intensity ratio (RIR) method, were obtained with the use of the PDXL2 integrated X-ray powder diffraction software (Ver. 2.8.4.0; Rigaku Corporation) [53].

The morphology and the elemental composition of the synthesized powders were determined using the SEM (JEOL JSM-6390 LV) coupled to electron dispersive spectroscopy (EDS, Oxford Instruments X-MaxN). The accelerating voltage in the SEM was in the range of 20–30 kV. The TEM analysis was conducted on a JEOL JEM-1400 Plus Electron microscope, with a voltage of 120 kV and a LaB_6 filament, at a magnification of 40,000x. ImageJ software was used for particle size distribution analysis.

To determine the silver content in the composites, the samples were prepared for ICP-OES analyses by dissolving 0.01 g of each sample in a hot solution consisting of 5 mL of concentrated nitric acid and 5 mL of water for 1 h. After cooling, the solution was filtered into a 25 mL volumetric flask. The silver ions release experiment was performed by preparing a dispersion of each sample (c = 0.002 g/mL) in deionized water. The obtained dispersions were kept at the ambient temperature for 24 h. The solution was collected after centrifugation and processed furtherly for ICP-OES measurements. The silver content was determined using an iCAP 6500 Duo ICP (Thermo Fisher Scientific, Cambridge, United Kingdom) optical emission spectrometer and analyzed with the iTEVA operational software. The solutions for calibration were prepared using Multi-Element Plasma Standard Solution 4, Specpure® (Alfa Aesar GmbH and Co KG, Germany). For each sample, the measurements were carried out in triplicates. The relative standard deviation was lower than 0.5%.

Zeta potentials of the TiO_2 and TiO_2/Ag samples were measured at room temperature in a disposable zeta cell (DTS 1060) of Nano ZS_{90} (Malvern, UK) apparatus. The measurements were performed under optimal scattering conditions applying 10 mg/L of each sample in deionized water. The measurements were started after the equilibration time of 5 min. UV–Vis spectroscopy data for all the investigated samples were collected on a Shimadzu UV – 3600 spectrophotometer. The UV-Vis spectra were obtained with the Shimadzu Integrating Sphere Attachment ISR- 3100 in the wavelength range of 250 nm to 900 nm with 1 nm resolution and medium averaging. The direct optical bandgaps were determined by creating the Tauc plot.

2.4. Antibacterial activity

The antibacterial activity was tested against two Gram-negative bacteria, namely *Escherichia coli* (ATCC 25922) and *Klebsiella pneumoniae* (ATCC 10031), and two Gram-positive bacteria, namely *Staphylococcus aureus* (ATCC 6538) and *Bacillus subtilis* (ATCC 6633), using the agar-well diffusion [54] and broth microdilution methods [55].

In the agar-well diffusion method, 90 mm diameter Petri dishes containing 22 mL of the nutrient agar (HiMedia, Mumbai, India) were seeded with 100 µL bacterial suspensions and the medium was allowed to solidify. The direct colony method was used for the preparation of bacterial suspensions. Suspension turbidity was conducted by comparison with 0.5 McFarland's standard and the inoculum size was adjusted so as to deliver a final inoculum of 10^8 colony forming units (CFU) per mL. A well with a diameter of 8 mm was then punched carefully using a sterile cork borer and 100 µL suspension of each test substance (30 mg/100 µL H_2O) was added to each labelled well. Amikacin in the amount of 30 µg/100 µL H_2O was used as a positive control, whereas 100 µL water served as a negative control. The same procedure was repeated for different microorganisms. After the inoculation of the organisms, compounds and controls, the plates were incubated for 24 h at 37 °C. Zones of inhibition were recorded in millimeters.

In the broth microdilution method, the minimum inhibitory concentration (MIC) for all the samples was determined by the Clinical and Laboratory Standards Institute (CLSI) reference method [56]. The 96-well microtiter plates were prepared by dispensing 100 µl of Mueller–Hinton broth into each well. Stock solutions of tested compounds (100 µL in 10% DMSO, 2 mg/mL) were pipetted into the first row of the plate, and double diluted by using the multichannel pipette. The direct colony method was used to prepare suspensions of bacteria in sterile 0.9% saline, and their turbidity evaluation was conducted by comparison with the 0.5 McFarland's standard. Finally, 10 µL of bacterial suspension (10^6 CFU/mL) was added into each well. The growth conditions and the sterility of the medium were checked, for each strain. The negative control was 10% DMSO, while erythromycin served as the positive control. All plates were placed in an incubator at 37°C for 24 hours. The bacterial growth was visualized by adding 10 µL of the 0.6% solution of resazurin. Wells where resazurin changed the color from blue to pink indicated viable bacterial cells. The MIC was defined as the lowest concentration of the tested compound at which no color change occurred.

3. Results and discussion

The XRPD patterns of TiO_2 and TiO_2 /Ag composites are presented in Fig. 1. The diffraction peaks of pure TiO_2 powders were similar to those of TiO_2 /Ag composites. All patterns contained diffraction peaks related to (1 0 1), (0 0 4), (2 0 0), (1 0 5), (2 1 1) and (2 0 4) planes of the anatase phase [30]. The relatively sharp peaks of anatase indicated a comparatively high level of structural order. The weight percentage of the rutile phase did not exceed 3% in any of the samples, as can be seen in Table 1. Mechanical activation preserved the biphasic nature of the material with the dominant presence of anatase, while structural defects were avoided. Interestingly, Pavlović et al. obtained a material with a significantly higher rutile amount (25%) than the one observed here, using the same activation time during the milling process [31]. This disparity appears to have been caused by the different powder-to-ball ratio used in this work, which has obviously led to dissimilar phase composition.

The main reflection of anatase, (1 0 1), was shifted to somewhat higher diffraction angles in the mechanically activated samples (Fig. 2). Because higher diffraction angles correspond to shorter distances between lattice planes, it can be inferred that compaction primarily occurred during the activation and not amorphization, given that the latter effect is most commonly paralleled with an increase in the bond lengths [57]. This is also corroborated by the diffractometric analysis, which showed no broadening of the diffraction lines to result from the

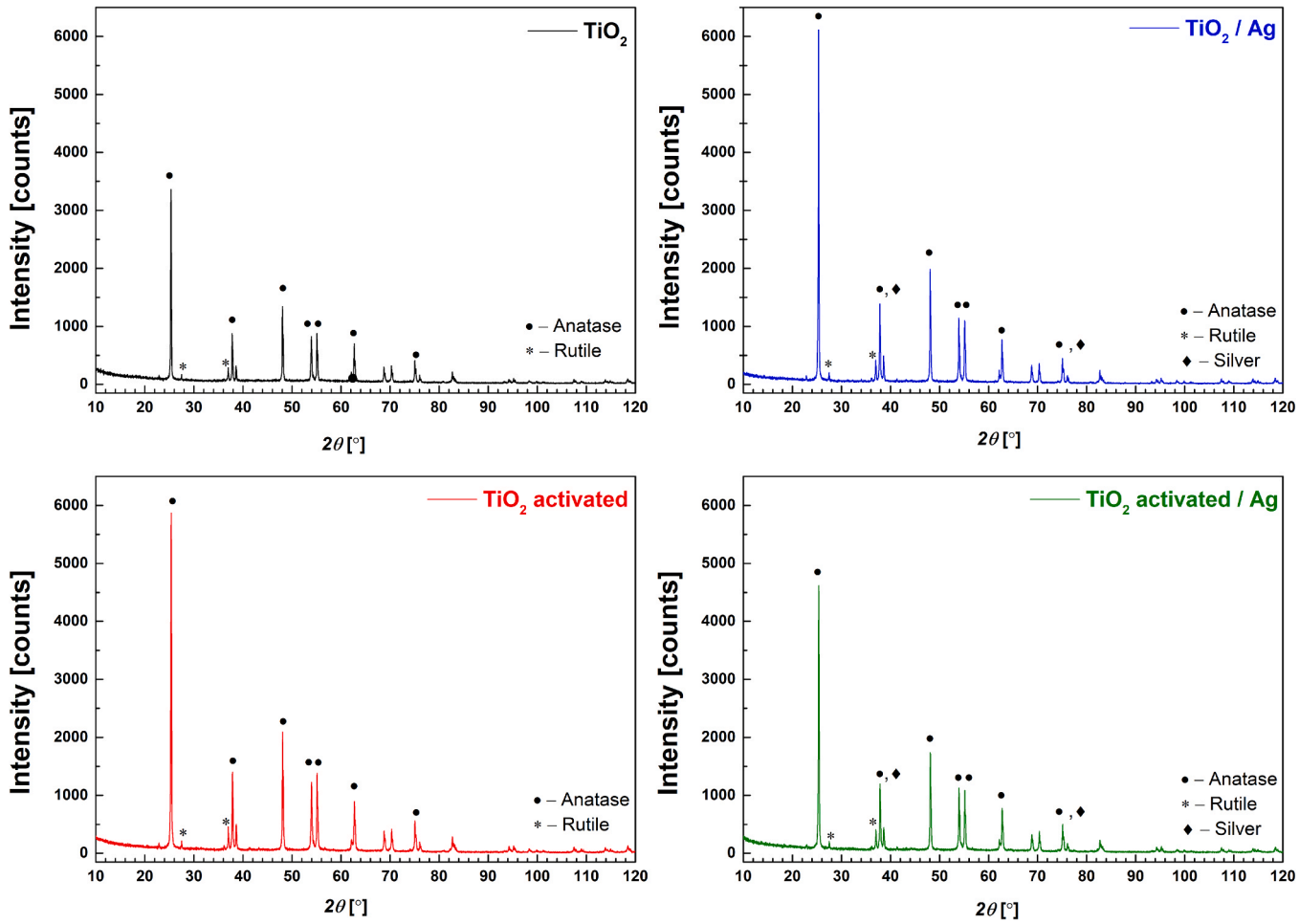

Fig. 1. XRPD patterns of the synthesized powders.

activation (Fig. 1). Likewise, the incorporation of the silver phase led to a shift of the reflections originating from anatase to higher diffraction angles (Fig. 2). The (2 0 0) reflection at ≈ 45° 2θ and the (2 2 0) reflection at ≈ 65° 2θ, corresponding to Ag, could not be clearly distinguished, the reason being the good dispersion of Ag particles in the TiO_2 matrix [58] and also the relatively low amount of Ag in the composites. Furthermore, the (1 1 1) silver peak at approximately 38° 2θ overlaps with the more intense (0 0 4) anatase peak [30,58]. As expected, the crystallite size of the anatase phase in mechanically activated samples was reduced relative to that in mechanically untreated samples (Table 1).

Surface morphology of the investigated powders was studied with the use of SEM, as shown in Fig. 3. For all four powders, a similar morphology was observed. The SEM micrographs for pure and silver-modified TiO_2 powders confirmed the presence of coexisting spherically shaped and polygonal particles. As a consequence of the high surface activity due to low particle size, all of the synthesized particles formed agglomerates. The presence of silver was observed in the EDS maps of TiO_2/Ag composites (Fig. 4), confirming that the modification of the TiO_2 matrix with silver was successful. A closer inspection of the EDS maps of the composites revealed that silver is uniformly dispersed across the entire surface or TiO_2 nanoparticle agglomerates. A homogeneous distribution of silver on the TiO_2 matrix is expected to be largely owing to the use of ultrasound during the synthesis procedure [59].

TEM images, along with the corresponding size distribution charts, are presented in Fig. 5. There is no obvious difference in particle size and shape between samples 1 and 2, which differ in terms of whether TiO_2 was activated or not. This implies that activation in the planetary ball mill did not affect gross morphological characteristics of TiO_2 particles significantly, just as it did not affect crystallinity (Fig. 1). In both cases, the average particle size was in the 100–120 nm range. On the other side, the introduction of silver had a notable influence on the particle size distribution. As we recently described in the report of a study dealing with hetero-nanocomposites containing iron oxide and silver nanoparticles [59], the reduction process led to the formation of silver nanoparticles larger than those comprising the metal oxide substrate. Further, as can be seen from size distribution charts for samples 3 and 4, the use of ultrasound during the chemical reduction caused the shift of the average particle size to a somewhat lower value (≈ 80 nm). This size reduction effect was clearly due to deagglomeration caused by the ultrasound.

The silver content was determined by ICP-OES for TiO_2/Ag and TiO_2 activated/Ag composites. The amount of 0.26 wt% was observed for TiO_2/Ag, while mechanical activation process led to a considerably higher amount of silver in the composite: 0.49 wt%. As per the preparation protocol specifics described earlier, a hypothetic 100% efficiency of capture of silver from the solution and into the solid phase would yield the amount in the composite of around 3.3 wt%. One order of magnitude lower amount of silver in the composites attests to the limited transformation of silver ion solutes into the precipitate on TiO_2. The mechanical activation, however, is expected to roughen the topmost atomic layer of the particle surface, if not increase the specific surface area, explaining the doubling of the amount of silver incorporable in the powder after this activation. The silver ions release from the structure was not confirmed because the silver amount was under the limits of detection.

Table 1
Phase composition of the synthesized materials. Next to the phase name, the crystal system and the space groups are presented, alongside the unit cell parameters, the crystallite sizes and the lattice strains for anatase, including the corresponding PDF card numbers from the ICDD database. Phase abundances are calculated by the RIR method.

Samples	Phase		
TiO_2	anatase *I4₁/amd* a = 3.7842(4) Å c = 9.511(2) Å V = 136.20(3) Å^3 PDF # 00–021–1272 96.9(3) %	rutile *P4₂/mnm* PDF # 01–075–1748 3.1(3) %	
Crystallite size [Å]	556(8)		
Lattice strain [%]	0.033(8)		
TiO_2 activated	anatase *I4₁/amd* a = 3.7834(5) Å c = 9.510(2) Å V = 136.13(4) Å^3 PDF # 00–021–1272 97.4(2) %	rutile *P4₂/mnm* PDF # 01–075–1748 2.6(2) %	
Crystallite size [Å]	484(8)		
Lattice strain [%]	0.03(1)		
TiO_2 / Ag	anatase *I4₁/amd* a = 3.7839(3) Å c = 9.509(1) Å V = 136.14(2) Å^3 PDF # 00–021–1272 97.1(1) %	rutile *P4₂/mnm* PDF # 01–075–1748 2.9(1) %	Ag *Fm-3 m* PDF # 01–087–0717 Near the limit of detection
Crystallite size [Å]	519(8)		
Lattice strain [%]	0		
TiO_2 activated / Ag	anatase *I4₁/amd* a = 3.7826(5) Å c = 9.507(2) Å V = 136.03(4) Å^3 PDF # 00–021–1272 97.0(2) %	rutile *P4₂/mnm* PDF # 01–075–1748 3.0(2) %	Ag *Fm-3 m* PDF # 01–087–0717 Near the limit of detection
Crystallite size [Å]	484(11)		
Lattice strain [%]	0.04(1)		

All of the investigated samples had similar negative values of zeta potential at neutral pH (Table 2), which is in accordance with the literature data for such systems [61–63]. However, the main obstacle for the confidence of deducing surface charges from the zeta potential values was agglomeration due to their ultrafine nature. Most bacteria exhibit negative zeta potentials when the pH is higher than 2 [64] and positively charged particle are therefore frequently favored as antimicrobials over their negatively charged counterparts. Here, however, it is worth reckoning that silver nanoparticles are typically less negatively charged than metal oxides [65], which allows for this electrostatic interaction with the bacterial surface to be slightly more favorable. Still, many studies have reported on an enhanced antimicrobial activity of slightly negatively charged nanoparticles [60,62], implying that chemistry and microstructure are more significant determinants of antibacterial activity than the surface charge.

To estimate the bandgap of the synthesized materials, Tauc plots were constructed and the typical extrapolation was performed. No

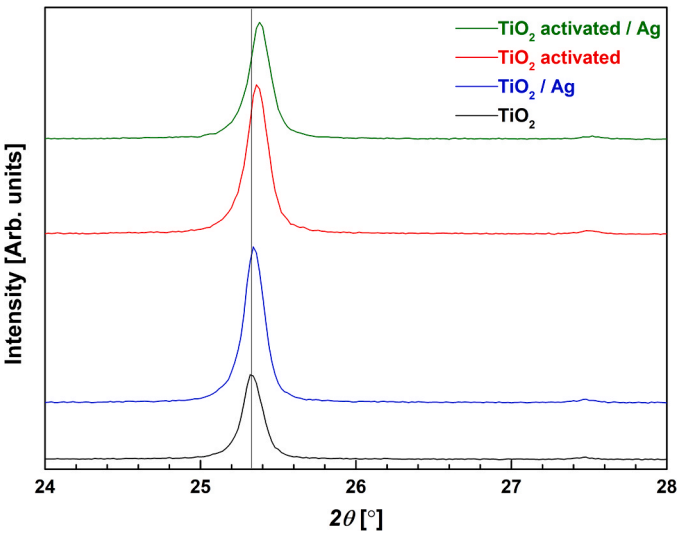

Fig. 2. The anatase (101) peak shifting to higher diffraction angles due to both mechanical activation and silver nanoparticle deposition.

significant changes were made to the bandgap of TiO_2 by either the mechanical activation or the addition of silver. Typically, mechanochemical treatments increase the number of defects in the surface layer of the material, such as Ti^{3+} and oxygen vacancies in TiO_2, leading to the narrowing of the bandgap [66]. The fact that the bandgap did not significantly change after the mechanical activation concurs with the earlier observed lack of reduced crystallinity (Fig. 1) and no evident morphological changes to the particles (Fig. 5) folllowing this activation.

In summary, as expected in an ideal scenario, mechanical activation influenced neither the microstructure nor the morphology, nor the bandgap. However, the milling process did lead to the doubling of the amount of silver incorporated into the anatase.

The antibacterial assays demonstrated that the mode of interaction between the particles and the bacterial cells is an important determinant of the antibacterial activity. This was concluded based on the different activities that emerged from the agar and the broth assays performed to assess these activities. Thus, in the agar assay, the commercial, non-activated TiO_2 displayed no inhibition zones and, therefore, had nil antibacterial activity. The mechanical activation of this powder, however, led to the inhibition zones that were 2–3 times lower than those of the positive controls, yet still considerable. The addition of silver to activated TiO_2 further increased the inhibition zones and it also imparted the antibacterial activity to non-activated TiO_2, which it would not have had in the absence of silver. Still, the higher activity of activated TiO_2 supplemented with silver than that of non-activated TiO_2 containing silver demonstrates that both mechanical activation and the addition of silver are positive contributors to the antibacterial activity in TiO_2. The antibacterial activity was not different for different species when no silver was added to the system. However, with the addition of silver, species selectivity was obtained, as the composites were more effective against the two Gram-negative species than against the two Gram-positive ones (Table 3).

In the broth assays, the results were less indicative of the effects of mechanical activation or phase composition than they were in the agar assay. The antibacterial activity was also markedly less pronounced than in the agar assay. This difference must be due to the limited dispersability of the particles, which preconditions their coming into contact with planktonic bacteria and exerting an effect of them. Because of this lower activity, as indicated by the typical MIC values of 0.25 mg/mL (Table 4), the effects of activation could not be delineated and the activation per se produced no measurable effect on the antibacterial activity. The addition of silver, however, did manage to considerably

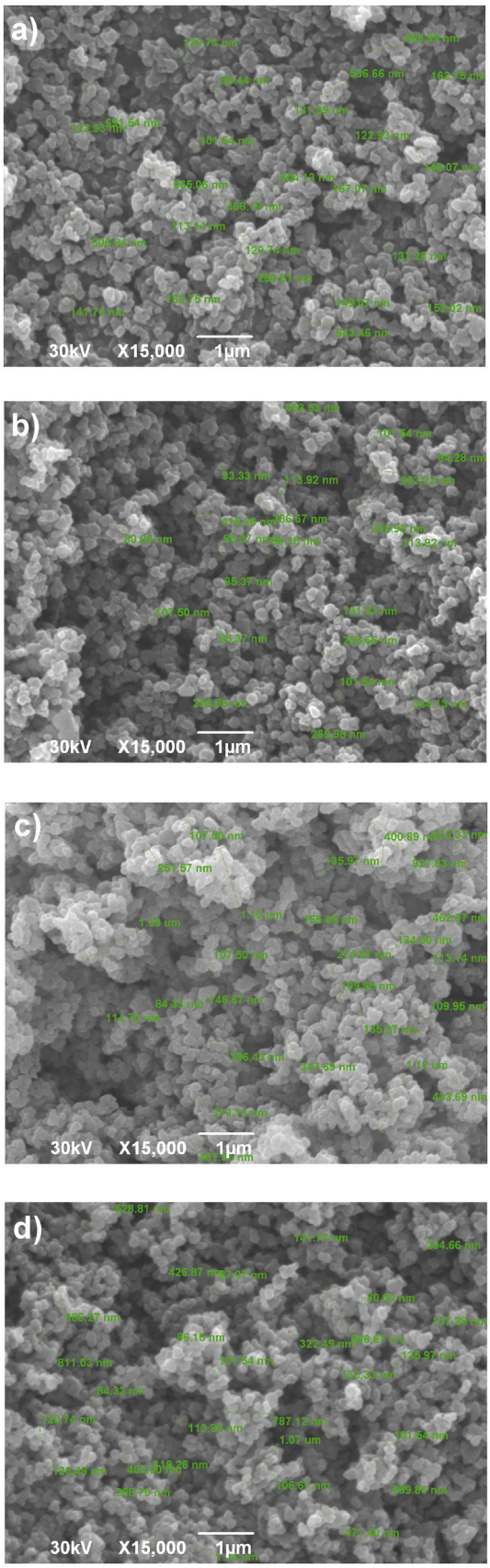

Fig. 3. SEM micrographs for all the synthesized samples – a) TiO_2; b) activated TiO_2; c) TiO_2/Ag; d) activated TiO_2/Ag.

lower the MIC against some species, such as *Bacillus subtilis* for both non-activated and activated TiO_2, and *Klebsiella pneumoniae* for activated TiO_2. In each of these cases, the antibacterial activity doubled with the addition of silver. Unlike in the agar assay, no clear Gram-negative vs. Gram-positive selectivity was obtained in the broth assay.

The mechanism of action is expected to be dominated by the attachment of the particles to the microbial cell walls, rather than by the silver ion release and their entrance to the bacterial cells to destroy them. This can be concluded from the fact that a considerably higher antibacterial activity was obtained in the agar assay than in the broth assay. Consequently, migration of the bacteria onto the surface of the material can be expected to represent a far more favorable condition for the interaction than the diffusion of the particles to the bacterial cells, especially since the diffusion of nanoparticles is comparatively slow. Contrary to an earlier developed composite of silver nanoparticles with TiO_2 [67], where an increase in the antibacterial activity was paralleled by an increase in the Ag ion release rate and an increased electron donor surface energy, in the systems investigated here the release of silver ions was not detected by ICP-OES. Furthermore, when the small silver particles are localized on the surface of TiO_2, the release of silver ions enables the bacterial growth inhibition [68], while in our case silver particles were much larger and partially incorporated in the structure, thus limiting their action through ion release effects.

4. Conclusions

Compositional and structural optimization of metal and metal oxide materials presents one of the most prospective paths for bringing the antibacterial activities thereof closer to those exhibited by small-molecule antibiotics. In this study, commercially available TiO_2 nanoparticles were mechanically activated and combined with silver through a simple physical reduction assisted with the ultrasound. This eco-friendly approach offers a considerable advantage compared to standard chemical procedures owing to its simplicity and avoidance of toxic substances. The resulting powders in various combinations (Ag *vs*. no Ag, activated *vs*. non-activated) were characterized using a range of experimental techniques. It was shown that mechanical activation did not reduce the particle size or crystallinity of TiO_2 nor did it consistently alter the bandgap, yet it enabled the doubling of the amount of silver incorporable into the material. The uniform distribution of silver across the volume of the composite is thought to have been due to the application of ultrasound in the silver deposition stage.

In addition to physicochemical characterization, the powders were assessed for their antibacterial activities. Both mechanical activation and silver addition in a rather moderate amount not exceeding 0.5 wt% augmented the antibacterial activity of anatase. The precursor TiO_2 powder produced no inhibition zone against any of the four bacterial species tested, while the mechanical activation of TiO_2 led to the formation of distinct inhibition zones against each of the four bacterial species tested. The addition of silver to activated TiO_2 further widened the inhibition zones and it also imparted the antibacterial activity to non-activated TiO_2. The highest activity, naturally, was observed for silver-supplemented activated TiO_2, for which it was on average only twice lower than that of the positive control. The antibacterial activity was not different for different species when no silver was added to the system. However, with the addition of silver, species selectivity was obtained, as the composites were more effective against the two Gram-negative species (*Escherichia coli* and *Klebsiella pneumoniae*) than against the two Gram-positive ones (*Staphylococcus aureus* and *Bacillus subtilis*). The antibacterial activity also increased with the addition of silver in the broth assay, but it was mediocre compared to that detected in the agar assay, attesting to the poor dispersability of the powders and their best performance when the bacterial cells migrate to the composite surface than *vice versa*. The absence of any detectable amount of release of silver ions was used to attribute the mechanism of antibacterial action of the composite to the direct interaction of the nanoparticles with the

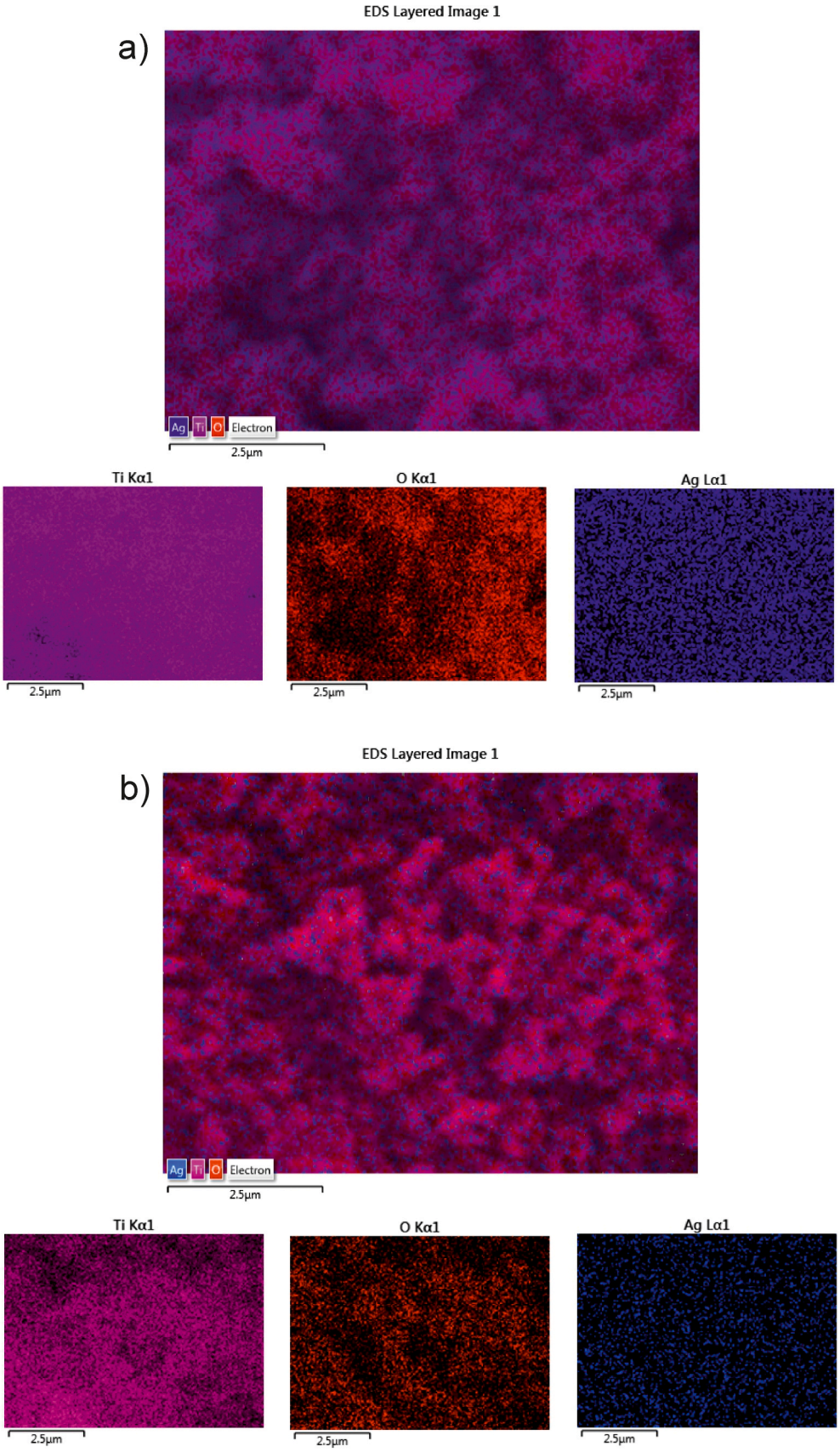

Fig. 4. EDS maps for TiO_2 /Ag composites – a) TiO_2 /Ag; b) activated TiO_2/Ag.

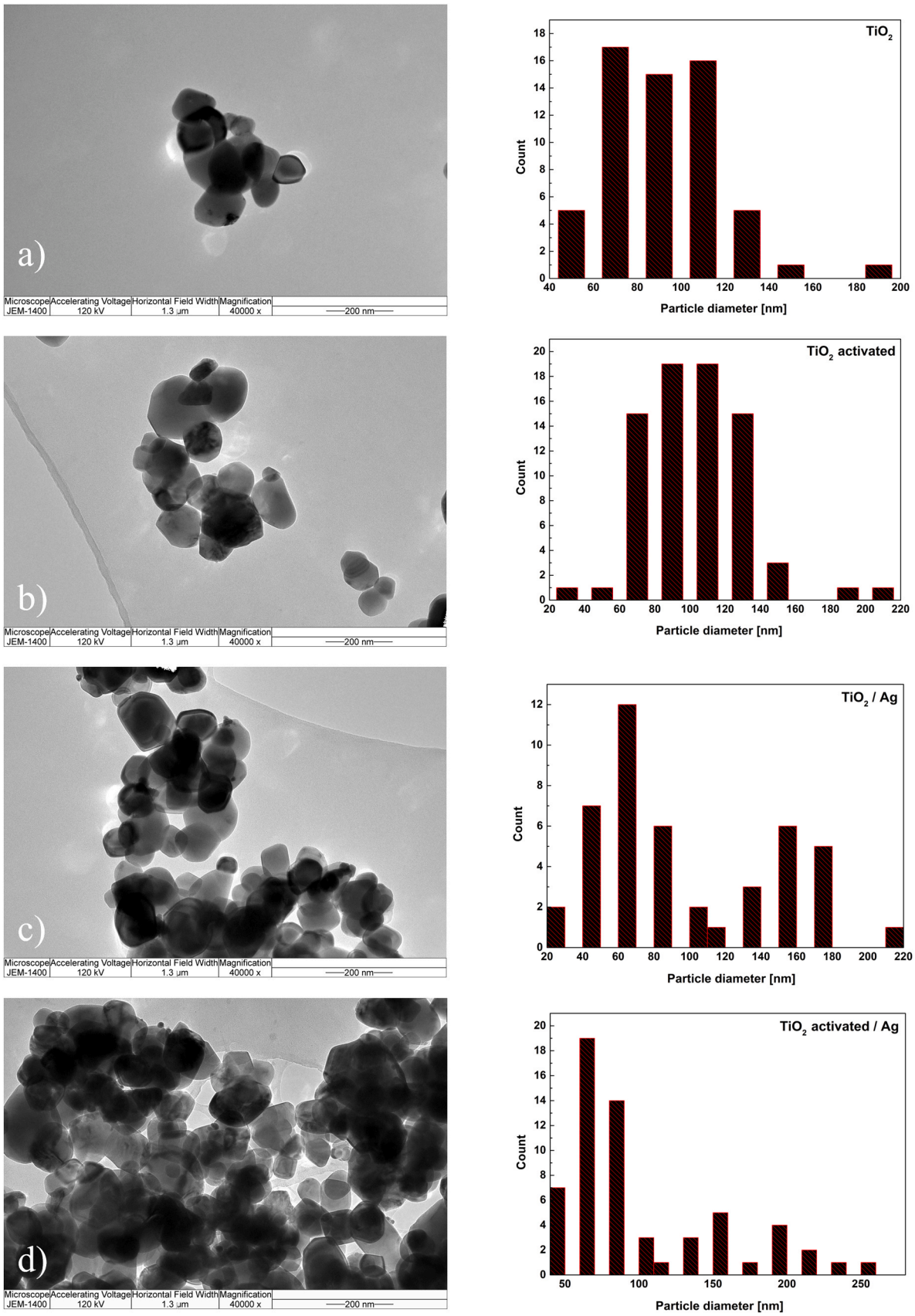

Fig. 5. TEM micrographs for all the synthesized samples – a) TiO_2; b) activated TiO_2; c) TiO_2 /Ag; d) activated TiO_2/Ag.

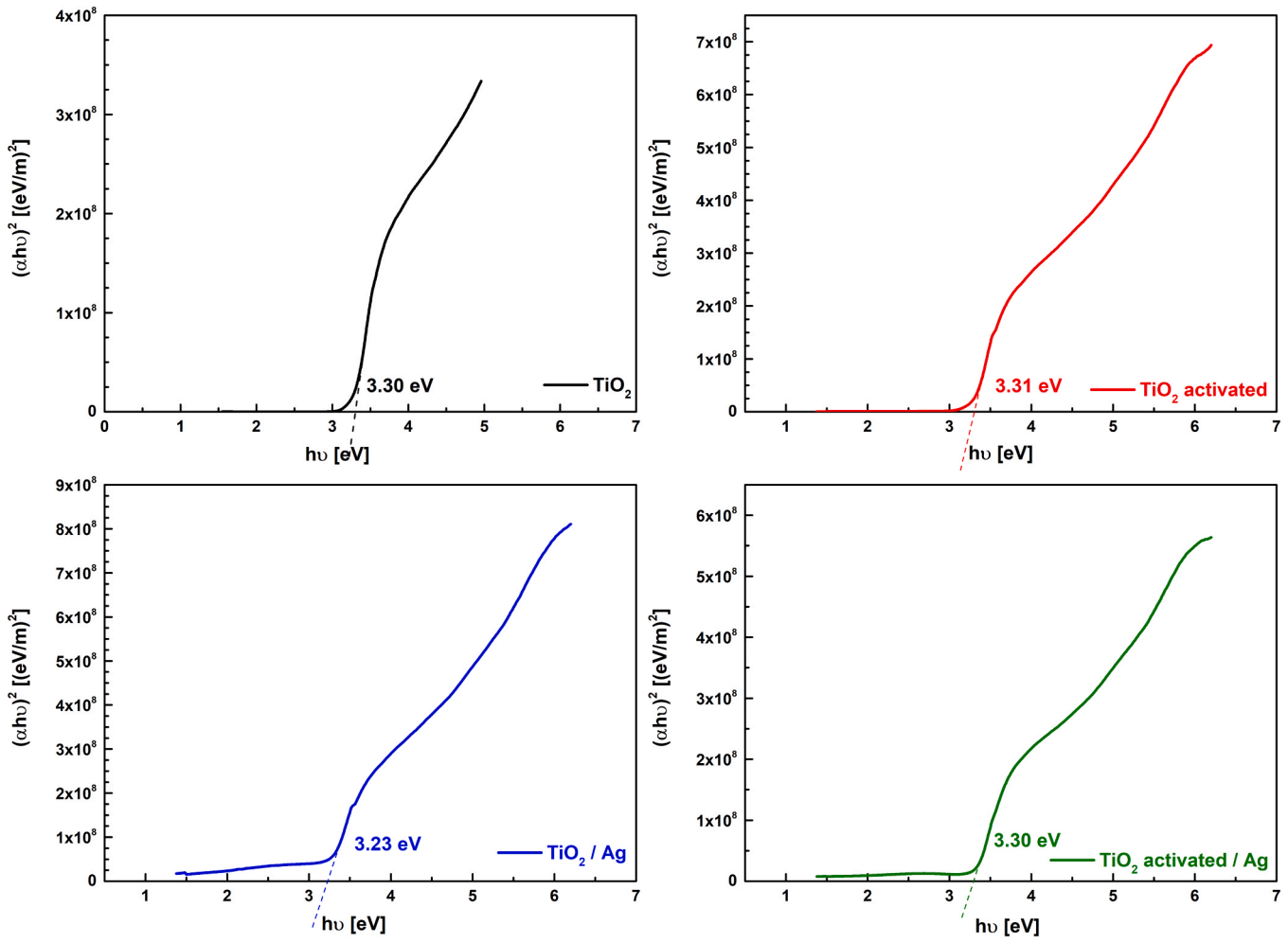

Fig. 6. Tauc plots and direct bandgaps of the synthesized powders.

Table 2
Mean values of zeta potential for TiO_2 and TiO_2/Ag samples measured under the standard conditions in deionized water.

Sample	Mean value	RSD [%]
TiO_2	-35.7	5.3
TiO_2 activated	-38.6	6.9
TiO_2/Ag	-36.6	5.4
TiO_2 activated/Ag	-31.8	6.9

Table 3
Zones of inhibition (mm) of the investigated samples.

	Escherichia coli	*Klebsiella pneumoniae*	*Staphylococcus aureus*	*Bacillus subtilis*
+ Control	20	26	18	26
TiO_2	/	/	/	/
TiO_2 activated	9	9	9	9
TiO_2 / Ag	11	10	9	9
TiO_2 activated / Ag	12	14	11	11

bacterial cell wall and the intracellular compartments. Overall, the fact that the boost in the antibacterial activity achieved by short mechanical activation of a metal oxide powder was of a similar magnitude as the boost obtained by the addition of silver is promising, as it gives hope that

Table 4
MICs (mg/mL) of the investigated samples.

	Escherichia coli	*Klebsiella pneumoniae*	*Staphylococcus aureus*	*Bacillus subtilis*
+ Control	0.03	0.03	0.06	0.06
TiO_2	0.25	0.25	0.25	0.25
TiO_2 activated	0.25	0.25	0.25	0.25
TiO_2 / Ag	0.25	0.25	0.25	0.125
TiO_2 activated / Ag	0.25	0.125	0.25	0.125

with appropriate microstructural alterations, the antibacterial activity of inorganic materials in general can be made comparable to that of small-molecule antibiotics. Future studies will continue to explore the structural modifications in metal/metal-oxide composites in search of a more superior antibacterial performance.

Declaration of Competing Interest

The authors declare that they have no known competing financial interests or personal relationships that could have appeared to influence the work reported in this paper.

Data availability

Data will be made available on request.

Acknowledgments

This research has been financially supported by the Ministry of Science, Technological Development and Innovation of Republic of Serbia (Contract No: 451–03–66/2024–03/200026, 451–03–66/2024–03/200116, 451–03–66/2024–03/200017, 451–03–66/2024–03/200168, 451–03–66/2024–03/200126).

Prime Novelty Statement

Titanium dioxide nanoparticles were mechanically activated and combined with particulate silver through chemical precipitation assisted with the ultrasound. The mechanical activation did not reduce the particle size or crystallinity of titanium dioxide nor did it consistently alter the bandgap, yet it enabled the doubling of the amount of silver distributed over the material. The uniform distribution of silver across the volume of the composite was achieved thanks to the application of ultrasound in the silver deposition stage. Both mechanical activation and silver addition in a rather moderate amount not exceeding 0.5 wt% augmented the antibacterial activity of the material. Although metals and metal oxides have subpar antibacterial activities compared to those of small-molecule antibiotics, there are hopes that with proper compositional and structural adjustments, as well as through the careful choice of the synthesis procedure, this gap might be bridged.

References

[1] E.D. Brown, G.D. Wright, Antibacterial drug discovery in the resistance era, Nature 529 (2016) 336–343, https://doi.org/10.1038/nature17042.
[2] C. Lim, E. Takahashi, M. Hongsuwan, V. Wuthiekanun, V. Thamlikitkul, S. Hinjoy, N.P. Day, S.J. Peacock, D. Limmathurotsakul, Epidemiology and burden of multidrug-resistant bacterial infection in a developing country, eLife 5 (2016) e18082, https://doi.org/10.7554/eLife.18082.
[3] L.L. Founou, R.C. Founou, S.Y. Essack, Antibiotic resistance in the food chain: a developing country-perspective, Front. Microbiol. 7 (2016), https://doi.org/10.3389/fmicb.2016.01881.
[4] J.A. Ayukekbong, M. Ntemgwa, A.N. Atabe, The threat of antimicrobial resistance in developing countries: causes and control strategies, Antimicrob. Resist. Infect. Control 6 (2017) 47, https://doi.org/10.1186/s13756-017-0208-x.
[5] European Centre for Disease Prevention and Control, Antimicrobial resistance in the EU/EEA (EARS-Net) - Annual Epidemiological Report 2019., Stockholm: ECDC, 2020. https://www.ecdc.europa.eu/en/publications-data/surveillance-antimicrobial-resistance-europe-2019 (accessed May 7, 2023).
[6] World Health Organization, Antimicrobial resistance: global report on surveillance, World Health Organization, Geneva, 2014. ⟨https://apps.who.int/iris/handle/10665/112642⟩.
[7] S. Parham, D.H.B. Wicaksono, S. Bagherbaigi, S.L. Lee, H. Nur, Antimicrobial treatment of different metal oxide nanoparticles: a critical review, J. Chin. Chem. Soc. 63 (2016) 385–393, https://doi.org/10.1002/jccs.201500446.
[8] A. Raghunath, E. Perumal, Metal oxide nanoparticles as antimicrobial agents: a promise for the future, Int. J. Antimicrob. Agents 49 (2017) 137–152, https://doi.org/10.1016/j.ijantimicag.2016.11.011.
[9] K. Gold, B. Slay, M. Knackstedt, A.K. Gaharwar, Antimicrobial activity of metal and metal-oxide based nanoparticles, Adv. Ther. 1 (2018) 1700033, https://doi.org/10.1002/adtp.201700033.
[10] A. Azam, A.S. Ahmed, M. Oves, M.S. Khan, S.S. Habib, A. Memic, Antimicrobial activity of metal oxide nanoparticles against Gram-positive and Gram-negative bacteria: a comparative study, Int. J. Nanomed. 7 (2012) 6003–6009, https://doi.org/10.2147/IJN.S35347.
[11] B. Lallo da Silva, M.P. Abuçafy, E. Berbel Manaia, J.A. Oshiro Junior, B.G. Chiari-Andréo, R.C.R. Pietro, L.A. Chiavacci, Relationship between structure and antimicrobial activity of zinc oxide nanoparticles: an overview, Int. J. Nanomed. 14 (2019) 9395–9410, https://doi.org/10.2147/IJN.S216204.
[12] Y. Li, C. Liao, S.C. Tjong, Recent advances in zinc oxide nanostructures with antimicrobial activities, Int. J. Mol. Sci. 21 (2020), https://doi.org/10.3390/ijms21228836.
[13] H. Mohd Yusof, R. Mohamad, U.H. Zaidan, N.A. Abdul Rahman, Microbial synthesis of zinc oxide nanoparticles and their potential application as an antimicrobial agent and a feed supplement in animal industry: a review, J. Anim. Sci. Biotechnol. 10 (2019) 57, https://doi.org/10.1186/s40104-019-0368-z.
[14] N.-Y.T. Nguyen, N. Grelling, C.L. Wetteland, R. Rosario, H. Liu, Antimicrobial activities and mechanisms of magnesium oxide nanoparticles (nMgO) against pathogenic bacteria, yeasts, and biofilms, Sci. Rep. 8 (2018) 16260, https://doi.org/10.1038/s41598-018-34567-5.
[15] A. Pugazhendhi, R. Prabhu, K. Muruganantham, R. Shanmuganathan, S. Natarajan, Anticancer, antimicrobial and photocatalytic activities of green synthesized magnesium oxide nanoparticles (MgONPs) using aqueous extract of Sargassum wightii, J. Photochem. Photobiol. B: Biol. 190 (2019) 86–97, https://doi.org/10.1016/j.jphotobiol.2018.11.014.
[16] G.S. El-Sayyad, F.M. Mosallam, A.I. El-Batal, One-pot green synthesis of magnesium oxide nanoparticles using Penicillium chrysogenum melanin pigment and gamma rays with antimicrobial activity against multidrug-resistant microbes, Adv. Powder Technol. 29 (2018) 2616–2625, https://doi.org/10.1016/j.apt.2018.07.009.
[17] A. Bouafia, S.E. Laouini, Plant-mediated synthesis of iron oxide nanoparticles and evaluation of the antimicrobial activity: a review, Mini-Rev. Org. Chem. 18 (2021) 725–734, https://doi.org/10.2174/1570193×17999200908091139.
[18] M. Jamzad, M. Kamari Bidkorpeh, Green synthesis of iron oxide nanoparticles by the aqueous extract of Laurus nobilis L. leaves and evaluation of the antimicrobial activity, J. Nanostructure Chem. 10 (2020) 193–201, https://doi.org/10.1007/s40097-020-00341-1.
[19] L. de, A.S. de Toledo, H.C. Rosseto, M.L. Bruschi, Iron oxide magnetic nanoparticles as antimicrobials for therapeutics, Pharm. Dev. Technol. 23 (2018) 316–323, https://doi.org/10.1080/10837450.2017.1337793.
[20] M. Aslam, A.Z. Abdullah, M. Rafatullah, Recent development in the green synthesis of titanium dioxide nanoparticles using plant-based biomolecules for environmental and antimicrobial applications, J. Ind. Eng. Chem. 98 (2021) 1–16, https://doi.org/10.1016/j.jiec.2021.04.010.
[21] S. Subhapriya, P. Gomathipriya, Green synthesis of titanium dioxide (TiO_2) nanoparticles by Trigonella foenum-graecum extract and its antimicrobial properties, Microb. Pathog. 116 (2018) 215–220, https://doi.org/10.1016/j.micpath.2018.01.027.
[22] C.L. de Dicastillo, C. Patiño, M.J. Galotto, Y. Vásquez-Martínez, C. Torrent, D. Alburquenque, A. Pereira, J. Escrig, Novel hollow titanium dioxide nanospheres with antimicrobial activity against resistant bacteria, Beilstein J. Nanotechnol. 10 (2019) 1716–1725, https://doi.org/10.3762/bjnano.10.167.
[23] V. Kumaravel, K.M. Nair, S. Mathew, J. Bartlett, J.E. Kennedy, H.G. Manning, B. J. Whelan, N.S. Leyland, S.C. Pillai, Antimicrobial TiO_2 nanocomposite coatings for surfaces, dental and orthopaedic implants, Chem. Eng. J. 416 (2021) 129071, https://doi.org/10.1016/j.cej.2021.129071.
[24] F.A. Bezza, S.M. Tichapondwa, E.M.N. Chirwa, Fabrication of monodispersed copper oxide nanoparticles with potential application as antimicrobial agents, Sci. Rep. 10 (2020) 16680, https://doi.org/10.1038/s41598-020-73497-z.
[25] H. Qamar, S. Rehman, D.K. Chauhan, A.K. Tiwari, V. Upmanyu, Green synthesis, characterization and antimicrobial activity of copper oxide nanomaterial derived from Momordica charantia, Int. J. Nanomed. 15 (2020) 2541–2553, https://doi.org/10.2147/IJN.S240232.
[26] M. Hashmi, S. Ullah, I.S. Kim, Copper oxide (CuO) loaded polyacrylonitrile (PAN) nanofiber membranes for antimicrobial breath mask applications, Curr. Res. Biotechnol. 1 (2019) 1–10, https://doi.org/10.1016/j.crbiot.2019.07.001.
[27] A.M. Shehabeldine, B.H. Amin, F.A. Hagras, A.A. Ramadan, M.R. Kamel, M. A. Ahmed, K.H. Atia, S.S. Salem, Potential antimicrobial and antibiofilm properties of copper oxide nanoparticles: time-kill kinetic essay and ultrastructure of pathogenic bacterial cells, Appl. Biochem. Biotechnol. 195 (2023) 467–485, https://doi.org/10.1007/s12010-022-04120-2.
[28] K.P. Priyanka, T.H. Sukirtha, K.M. Balakrishna, T. Varghese, Microbicidal activity of TiO2 nanoparticles synthesised by sol–gel method, IET Nanobiotechnol. 10 (2016) 81–86, https://doi.org/10.1049/iet-nbt.2015.0038.
[29] M. Ghosh, M. Mondal, S. Mandal, A. Roy, S. Chakrabarty, G. Chakrabarti, S. K. Pradhan, Enhanced photocatalytic and antibacterial activities of mechanosynthesized TiO2–Ag nanocomposite in wastewater treatment, J. Mol. Struct. 1211 (2020) 128076, https://doi.org/10.1016/j.molstruc.2020.128076.
[30] O. Akhavan, Lasting antibacterial activities of Ag– TiO_2/Ag/a- TiO_2 nanocomposite thin film photocatalysts under solar light irradiation, J. Colloid Interface Sci. 336 (2009) 117–124, https://doi.org/10.1016/j.jcis.2009.03.018.
[31] V.P. Pavlović, J.D. Vujančević, P. Mašković, J. Ćirković, J.M. Papan, D. Kosanović, M.D. Dramićanin, P.B. Petrović, B. Vlahović, V.B. Pavlović, Structure and enhanced antimicrobial activity of mechanically activated nano TiO_2, J. Am. Ceram. Soc. 102 (2019) 7735–7745, https://doi.org/10.1111/jace.16668.
[32] S. Palmas, A.M. Polcaro, J.R. Ruiz, A. Da Pozzo, A. Vacca, M. Mascia, F. Delogu, P. C. Ricci, Effect of the mechanical activation on the photoelectrochemical properties of anatase powders, Int. J. Hydrog. Energy 34 (2009) 9662–9670, https://doi.org/10.1016/j.ijhydene.2009.07.058.
[33] D. Dvoranová, V. Brezová, M. Mazúr, M.A. Malati, Investigations of metal-doped titanium dioxide photocatalysts, Appl. Catal. B: Environ. 37 (2002) 91–105, https://doi.org/10.1016/S0926-3373(01)00335-6.
[34] P. Ribao, J. Corredor, M.J. Rivero, I. Ortiz, Role of reactive oxygen species on the activity of noble metal-doped TiO2 photocatalysts, J. Hazard. Mater. 372 (2019) 45–51, https://doi.org/10.1016/j.jhazmat.2018.05.026.
[35] S.I. Mogal, M. Mishra, V.G. Gandhi, R.J. Tayade, Metal doped titanium dioxide: synthesis and effect of metal ions on physico-chemical and photocatalytic properties, Mater. Sci. Forum 734 (2013) 364–378, https://doi.org/10.4028/www.scientific.net/MSF.734.364.
[36] J. Prakash, S. Sun, H.C. Swart, R.K. Gupta, Noble metals- TiO_2 nanocomposites: from fundamental mechanisms to photocatalysis, surface enhanced Raman scattering and antibacterial applications, Appl. Mater. Today 11 (2018) 82–135, https://doi.org/10.1016/j.apmt.2018.02.002.

[37] P.D. Cozzoli, E. Fanizza, R. Comparelli, M.L. Curri, A. Agostiano, D. Laub, Role of metal nanoparticles in TiO_2/Ag nanocomposite-based microheterogeneous photocatalysis, J. Phys. Chem. B 108 (2004) 9623–9630, https://doi.org/10.1021/jp0379751.
[38] K. Kočí, K. Matějů, L. Obalová, S. Krejčíková, Z. Lacný, D. Plachá, L. Čapek, A. Hospodková, O. Šolcová, Effect of silver doping on the TiO_2 for photocatalytic reduction of TiO_2, Appl. Catal. B: Environ. 96 (2010) 239–244, https://doi.org/10.1016/j.apcatb.2010.02.030.
[39] M.S. Lee, S.-S. Hong, M. Mohseni, Synthesis of photocatalytic nanosized TiO_2–Ag particles with sol–gel method using reduction agent, J. Mol. Catal. A: Chem. 242 (2005) 135–140, https://doi.org/10.1016/j.molcata.2005.07.038.
[40] K. Zheng, M.I. Setyawati, D.T. Leong, J. Xie, Antimicrobial silver nanomaterials, Coord. Chem. Rev. 357 (2018) 1–17, https://doi.org/10.1016/j.ccr.2017.11.019.
[41] S. Parmar, H. Kaur, J. Singh, A.S. Matharu, S. Ramakrishna, M. Bechelany, Recent advances in green synthesis of Ag NPs for extenuating antimicrobial resistance, Nanomaterials 12 (2022), https://doi.org/10.3390/nano12071115.
[42] V.K. Sharma, R.A. Yngard, Y. Lin, Silver nanoparticles: Green synthesis and their antimicrobial activities, Adv. Colloid Interface Sci. 145 (2009) 83–96, https://doi.org/10.1016/j.cis.2008.09.002.
[43] G.A. Sotiriou, S.E. Pratsinis, Antibacterial activity of nanosilver ions and particles, Environ. Sci. Technol. 44 (2010) 5649–5654, https://doi.org/10.1021/es101072s.
[44] A. Katsumiti, D. Gilliland, I. Arostegui, M.P. Cajaraville, Mechanisms of toxicity of ag nanoparticles in comparison to bulk and ionic Ag on mussel hemocytes and gill cells, PLOS ONE 10 (2015) e0129039, https://doi.org/10.1371/journal.pone.0129039.
[45] Y. Xiong, M. Brunson, J. Huh, A. Huang, A. Coster, K. Wendt, J. Fay, D. Qin, The role of surface chemistry on the toxicity of Ag nanoparticles, Small 9 (2013) 2628–2638, https://doi.org/10.1002/smll.201202476.
[46] P.V. AshaRani, G. Low Kah Mun, M.P. Hande, S. Valiyaveettil, Cytotoxicity and genotoxicity of silver nanoparticles in human cells, ACS Nano 3 (2009) 279–290, https://doi.org/10.1021/nn800596w.
[47] M. Ahamed, M.S. AlSalhi, M.K.J. Siddiqui, Silver nanoparticle applications and human health, Clin. Chim. Acta 411 (2010) 1841–1848, https://doi.org/10.1016/j.cca.2010.08.016.
[48] C.-Ş. Adochiţe, C. Vițelaru, A.C. Parau, A.E. Kiss, I. Pană, A. Vlădescu, S. Costinaș, M. Moga, R. Muntean, M. Badea, M. Idomir, Synthesis and investigation of antibacterial activity of thin films based on TiO_2-Ag and TiO_2-Ag with potential applications in medical environment, Nanomaterials 12 (2022), https://doi.org/10.3390/nano12060902.
[49] H. Zhang, G. Chen, Potent antibacterial activities of Ag/TiO_2 nanocomposite powders synthesized by a one-pot Sol−Gel method, Environ. Sci. Technol. 43 (2009) 2905–2910, https://doi.org/10.1021/es803450f.
[50] D. Lin, Y. Yang, J. Wang, W. Yan, Z. Wu, H. Chen, Q. Zhang, D. Wu, W. Qin, Z. Tu, Preparation and characterization of TiO_2-Ag loaded fish gelatin-chitosan antibacterial composite film for food packaging, Int. J. Biol. Macromol. 154 (2020) 123–133, https://doi.org/10.1016/j.ijbiomac.2020.03.070.
[51] S.A. Amin, M. Pazouki, A. Hosseinnia, Synthesis of TiO_2–Ag nanocomposite with sol–gel method and investigation of its antibacterial activity against E. coli, Powder Technol. 196 (2009) 241–245, https://doi.org/10.1016/j.powtec.2009.07.021.
[52] B.S. Necula, L.E. Fratila-Apachitei, S.A.J. Zaat, I. Apachitei, J. Duszczyk, In vitro antibacterial activity of porous TiO_2–Ag composite layers against methicillin-resistant Staphylococcus aureus, Acta Biomater. 5 (2009) 3573–3580, https://doi.org/10.1016/j.actbio.2009.05.010.
[53] R.S. André, C.A. Zamperini, E.G. Mima, V.M. Longo, A.R. Albuquerque, J. R. Sambrano, A.L. Machado, C.E. Vergani, A.C. Hernandes, J.A. Varela, E. Longo, Antimicrobial activity of TiO_2:Ag nanocrystalline heterostructures: Experimental and theoretical insights, Chem. Phys. 459 (2015) 87–95, https://doi.org/10.1016/j.chemphys.2015.07.020.
[54] Rigaku, Rigaku, Tokyo, Japan, PDXL Integr. X-Ray Powder Diffr. Softvare (2011).
[55] C. Perez, M. Pauli, P. Bazerque, An antibiotic assay by agar well diffusion method, Acta Biol. Et. Med. Exp. 15 (1990) 113–115.
[56] European Committee for Antimicrobial Susceptibility Testing (EUCAST) of the European Society of Clinical Microbiology and Infectious Diseases (ESCMID), Determination of minimum inhibitory concentrations (MICs) of antibacterial agents by broth dilution, Clin. Microbiol. Infect. 9 (2003) ix–xv, https://doi.org/10.1046/j.1469-0691.2003.00790.x.
[57] National Committee for Clinical Laboratory Standards, Approval Standard Document M7-A5, (2000).
[58] V. Uskoković, Disordering the disorder as the route to a higher order: incoherent crystallization of calcium phosphate through amorphous precursors, Cryst. Growth Des. 19 (2019) 4340–4357, https://doi.org/10.1021/acs.cgd.9b00061.
[59] C.-C. Chang, J.-Y. Chen, T.-L. Hsu, C.-K. Lin, C.-C. Chan, Photocatalytic properties of porous TiO2/Ag thin films, Thin Solid Films 516 (2008) 1743–1747, https://doi.org/10.1016/j.tsf.2007.05.033.
[60] M. Šuljagić, M. Milenković, V. Uskoković, M. Mirković, B. Vrbica, V. Pavlović, V. Živković-Radovanović, D. Stanković, L. Andjelković, Silver distribution and binding mode as key determinants of the antimicrobial performance of iron oxide/silver nanocomposites, Mater. Today Commun. 32 (2022) 104157, https://doi.org/10.1016/j.mtcomm.2022.104157.
[61] A. Azouri, M. Ge, K. Xun, K. Sattler, J. Lichwa, C. Ray, Zeta potential studies of titanium dioxide and silver nanoparticle composites in water-based colloidal suspension, in: MN2006, Multifunctional Nanocomposites, 2006, pp. 221–223, https://doi.org/10.1115/MN2006-17072.
[62] W.-C. Lin, C.-N. Chen, T.-T. Tseng, M.-H. Wei, J.H. Hsieh, W.J. Tseng, Micellar layer-by-layer synthesis of TiO_2/Ag hybrid particles for bactericidal and photocatalytic activities, J. Eur. Ceram. Soc. 30 (2010) 2849–2857, https://doi.org/10.1016/j.jeurceramsoc.2009.12.016.
[63] A.K. Behera, K.P. Shadangi, P.K. Sarangi, Synthesis of dye-sensitized TiO_2/Ag doped nano-composites using UV photoreduction process for phenol degradation: a comparative study, Environ. Pollut. 312 (2022) 120019, https://doi.org/10.1016/j.envpol.2022.120019.
[64] A.P.V. Ferreyra Maillard, J.C. Espeche, P. Maturana, A.C. Cutro, A. Hollmann, Zeta potential beyond materials science: Applications to bacterial systems and to the development of novel antimicrobials, Biochim. Et. Biophys. Acta (BBA) - Biomembr. 1863 (2021) 183597, https://doi.org/10.1016/j.bbamem.2021.183597.
[65] K. Pušnik Črešnar, A. Aulova, D.N. Bikiaris, D. Lambropoulou, K. Kuzmič, L. Fras Zemljič, Incorporation of metal-based nanoadditives into the PLA matrix: effect of surface properties on antibacterial activity and mechanical performance of PLA nanoadditive films, Molecules 26 (2021), https://doi.org/10.3390/molecules26144161.
[66] K. Kucio, V. Sydorchuk, S. Khalameida, B. Charmas, The effect of mechanochemical, microwave and hydrothermal modification of precipitated TiO_2 on its physical-chemical and photocatalytic properties, J. Alloy. Compd. 862 (2021) 158011, https://doi.org/10.1016/j.jallcom.2020.158011.
[67] C. Liu, L. Geng, Y. Yu, Y. Zhang, B. Zhao, Q. Zhao, Mechanisms of the enhanced antibacterial effect of Ag- TiO_2 coatings, Biofouling 34 (2018) 190–199, https://doi.org/10.1080/08927014.2017.1423287.
[68] X.H. Yang, H.T. Fu, X.C. Wang, J.L. Yang, X.C. Jiang, A.B. Yu, Synthesis of silver-titanium dioxide nanocomposites for antimicrobial applications, J. Nanopart. Res. 16 (2014) 2526, https://doi.org/10.1007/s11051-014-2526-8.